CLINICAL APPLICATIONS OF ARTIFICIAL INTELIGENCE IN PET OF LUNG CANCER

Katherine A. Zukotynski, MD, PhD, FRCPC
Departments of Medicine and Radiology
McMaster University
1200 Main St. W., Hamilton, ON L9G 4X5, Canada
Email: katherine.zukotynski@utoronto.ca
Tel. 905-521-2100 x 76556

Vincent C. Gaudet, PhD
Departments of Electrical and Computer Engineering
University of Waterloo
Email: vcgaudet@uwaterloo.ca

Carlos F. Uribe, PhD
PET Functional Imaging, BC Cancer, Vancouver, BC, Canada
Email: curibe@bccrc.ca

Katarina Chiam
Division of Engineering Science
University of Toronto
Email: katarina.chiam@mail.utoronto.ca

François Bénard, MD, FRCPC
Department of Radiology
University of British Columbia
Email: fbenard@bccrc.ca

Victor H. Gerbaudo, PhD, MSHCA
Department of Radiology
Brigham and Women's Hospital and Harvard Medical School
75 Francis Street, Boston, Massachusetts 02492, USA
E-mail: gerbaudo@bwh.harvard.edu
Tel. 617-732-6290

Corresponding author: Dr. Katherine A. Zukotynski

Please note that Dr. Zukotynski, Dr. Gaudet, Dr. Uribe, Dr. Bénard, Ms. Chiam and Dr. Gerbaudo have nothing to disclose.

Synopsis: The ability of a computer to perform tasks normally requiring human intelligence or *artificial intelligence* (AI) is not new. However, until recently, practical applications in medical imaging were limited, especially in the clinic. With advances in theory, microelectronic circuits and computer architecture as well as our ability to acquire and access large amounts of data, AI is becoming increasingly ubiquitous in medical imaging. Of particular interest to our community, *radiomics* tries to identify imaging features of specific pathology that can represent for example the texture or shape of a region in the image. This is done based on a review of mathematical patterns and pattern combinations. The difficulty is often finding sufficient data to span the spectrum of disease heterogeneity since many features change with pathology as well as over time and, among other issues, data acquisition is expensive. Although we are currently in the early days of the practical application of AI to medical imaging, research is ongoing to integrate imaging, molecular pathobiology, genetic make-up and clinical manifestations to classify patients into subgroups for the purpose of precision medicine, or in other words, predicting *a priori* treatment response and outcome. Lung cancer is a functionally and morphologically heterogeneous disease. Positron emission tomography (PET) is an imaging technique with an important role in the precision medicine of lung cancer patients that helps predict early response to therapy and guides the selection of appropriate treatment. Although still in its infancy, early results suggest the use of AI in PET of lung cancer has promise for the detection, segmentation and characterization of disease as well as for outcome prediction.

Key Words: Lung cancer; Positron Emission Tomography; pulmonary nodule; cancer diagnosis; targeted therapy, artificial intelligence

Key Points:

1. AI is helpful to detect, segment and characterize pulmonary nodules on CT and PET.
2. AI is a helpful adjunct for PET as a predictive and prognostic biomarker in lung cancer patients.
3. Clinical applications of AI in PET of lung cancer patients span the spectrum of initial and subsequent treatment strategy, including staging, detecting recurrence and predicting outcomes.

Lung Cancer, Precision Medicine and Positron Emission Tomography

Lung cancer is the second most diagnosed malignancy according to the American Cancer Society, accounting for approximately 228,820 new cases and 135,720 deaths in the United States in 2020 (1). While localized disease may be curable, systemic disease is the leading cause of cancer-related death, surpassing death from breast, prostate and colorectal cancer combined.

Lung cancer is classified into: 1. non-small cell lung cancer (NSCLC) and 2. small cell lung cancer (SCLC) (2). Treatment options include surgery, radiotherapy, chemotherapy, immunotherapy, and targeted medications including epidermal growth factor receptor (EGFR) inhibitors and others directed to genetic mutations (e.g. ALK, ROS1), among others. Integration of clinical, genomic and imaging findings may help personalize lung cancer management (2,3) and has the potential to identify appropriate treatment to maximize patient benefit while limiting toxicity.

Positron emission tomography (PET) plays a key role in lung cancer imaging, both at the time of initial staging and subsequent treatment planning. The true strength of PET lies in its ability to detect distant metastatic disease as well as to non-invasively characterize tumor heterogeneity throughout the body over time. It can provide predictive and prognostic insight into therapy response and identify sites of disease harboring clonal proliferations of cells resistant to treatment such that timely treatment changes can be made. Currently, PET scanners incorporate either computed tomography (CT) or magnetic resonance imaging (MRI). PET/CT is more common than PET/MR in routine clinical practice; however, both are helpful for the assessment of patients with lung cancer. Also, there are several radiopharmaceuticals that may be used to image lung cancer with PET. The most ubiquitous PET radiopharmaceutical in oncology is ^{18}F-labeled 2-fluoro-2-deoxy-D-glucose ([^{18}F]FDG), a glucose analogue that is preferentially taken up by cancer cells (4,5). Several other PET radiopharmaceuticals may be helpful for lung cancer imaging such as [^{18}F]fluoroazomycin arabinofuranoside (FAZA) and [^{18}F]fluoromisonidazole(1-(2-nitroimidazolyl)-2-hydroxy-3-fluoropropane (FMISO) for targeting hypoxia, and the quinoline-based ligands for evaluating cancer-associated fibroblasts (fibroblast activating protein inhibitors or FAPI), among others (6,7). To date, no radiopharmaceutical is specific for lung cancer and uptake can also occur in non-lung cancer malignancy or non-malignant causes. Further, the intensity of uptake depends on several factors in addition to pathology, such as uptake time and other technical parameters. Ultimately, clinical context is key for image interpretation.

AI applications may be helpful across the spectrum of lung cancer (from localized through widespread disease) both at the time of initial and subsequent treatment strategy, for several tasks including disease detection/ staging, segmentation and response prediction, among other tasks.

Current Clinical Value of PET and AI in Pulmonary Nodules and Lung Cancer Staging

A solitary pulmonary nodule (SPN) is defined as being less than 3 cm in size and may be either solid or subsolid (8). The risk that an incidentally detected SPN to be malignant is related to several factors, such as the patient age, smoking history, and appearance on CT. PET/CT is not included in the work-up of subsolid nodules, due to their low metabolic activity and risk of false-negative results. In this case, the Fleishner Society guidelines recommend follow up with CT to check for lesion stability, and imaging surveillance for up to 5 years as needed (9). However, one of the most common clinical indications for PET is the evaluation of a solitary solid pulmonary nodule that is indeterminate for malignancy based on clinical parameters and diagnostic imaging. [^{18}F]FDG-PET/CT is very accurate to characterize a solid SPN as malignant, with high negative predictive value to exclude cancer in nodules larger than 8 mm (10-13). Also, if a nodule is known to be malignant, the more intensely [^{18}F]FDG-avid the nodule is, the more aggressive the disease tends to be. [^{18}F]FDG-PET/CT is also helpful for lung cancer staging. [^{18}F]FDG-PET/CT is used to: 1) characterize indeterminate solitary solid pulmonary nodules over 8 mm on anatomic imaging; 2) guide biopsy to the site of most aggressive disease, and 3) evaluate disease extent including local, regional and distant spread. Since certain lung cancer subtypes, such as carcinoid, may have low metabolic activity, while benign processes, such as infection or inflammation, may be intensely [^{18}F]FDG-avid, either follow-up imaging or tissue sampling is typically needed for further characterization. Ultimately, the post [^{18}F]FDG-PET/CT risk of malignancy is used to guide clinical decisions such as CT surveillance, biopsy and/ or surgical resection. For example, an indeterminate SPN on CT with a low probability of lung cancer prior to PET/CT, and low [^{18}F]FDG avidity, indicates observation may be the most appropriate management. In contrast to this, an indeterminate SPN on CT but with intense [^{18}F]FDG uptake indicates biopsy is necessary, with surgical resection if this is the only site of malignant disease. According to Society of Nuclear Medicine and Molecular Imaging (SNMMI), [^{18}F]FDG-PET/CT is helpful to: 1) detect a potentially malignant SPN early permitting curative surgery in high-risk patients, 2) exclude malignancy in low-risk patients with a questionable lesion, and 3) improve outcomes by avoiding unnecessary surgery (14).

In addition to lung nodule characterization, PET is helpful for lung cancer staging by providing complementary metabolic information to the anatomic information in CT (15). [^{18}F]FDG-PET/CT helps detect malignant tissue differentiating it from adjacent benign findings (16). For *lymph node* disease (N status), [^{18}F]FDG-PET/CT is more accurate than CT for evaluating

disease spread (17). False-negative results may be encountered however, such as lesions that are too small to be detected by the scanner or those that are not metabolically active. On the other hand, false-positive results may occur with inflammation or infection. Therefore, tissue sampling is typically needed for lesion characterization (18). The sensitivity, specificity and accuracy of [^{18}F]FDG-PET/CT for detecting *distant metastases* (M status) is very high (19, 20).

Utility of AI in conjunction with PET in lung nodules and lung cancer:

Research into the clinical applications of AI involving PET in patients with lung cancer have increased dramatically in recent years. This has largely resulted from improved electronics and software as well as access to databases containing large imaging datasets that can be used for training of the AI models; for example, the Lung Image Database Consortium and Image Database Resource Initiative (LIDC-IRDI), the US National Lung Screening Trial (NLST) and the Dutch-Belgian Lung Cancer Screening trial (NELSON), among others (21-24). Although these databases have made research more ubiquitous, the available data is still limited in many ways. For example, while the LIDC-IRDI database comprises chest CT studies with a spectrum of benign through malignant findings including lung cancer and metastatic disease, very few cases have histologic confirmation or a 2-year follow-up. In addition, for supervised AI algorithms, performance is tied to the gold standard, which is often the annotation of an expert (e.g. a radiologist or a nuclear medicine physician), and as such remains imperfect.

Perhaps the most common clinical applications of AI in lung cancer are in the areas of nodule/disease detection. In general, these studies have concentrated on the use of CT, and have suggested that computer algorithms improve detection and assessment and may positively impact patient care (25). However, there have been a few studies focused on the use of PET. While often retrospective and including small numbers of subjects, these studies suggest that AI is helpful, albeit with performance closely tied to technical parameters. A retrospective study by Schwyzer et al. of 57 subjects with 92 [^{18}F]FDG-avid pulmonary nodules using a deep learning algorithms, gave an area under the curve (AUC) for lung nodule detection of 0.796 [Confidence Interval (CI) 95%; 0.772-0.869] when ordered subset expectation maximization (OSEM) reconstruction was selected. The algorithm performance improved to an AUC=0.848 (CI 95%; 0.828-0.869) with block sequential regularized expectation maximization (BSREM) reconstruction (26). Another retrospective study by Schwyzer et al. of 100 subjects who had PET/CT, 50 with lung cancer ranging from stage I to stage IV disease and 50 without lung lesions, showed a deep learning algorithm had sensitivity of 95.9% and specificity of 91.5% to discriminate lung cancer patients from normal controls. This decreased slightly with lower injected activity (27). A deep learning

approach based on individual convolutional neural networks (CNNs) for CT and PET, followed by fusion of the results, was used for segmentation in lung cancer (Fig. 1) (28). Of note, accurate assessment of disease extent remains challenging when pathology abuts soft tissue of similar density, such as the pleura or blood vessels.

There have also been several studies using AI for lung cancer staging. For example, a study by Kirienko et al. of 472 patients imaged with PET/CT, of which 353 had T1-T2 disease and 119 T3-T4 tumors, achieved 69% accuracy using a convolutional neural network (CNN) to classify subjects as having either T1-T2 disease or T3-T4 lung cancer (29). A study by Tau et al. found the sensitivity, specificity and accuracy were 0.74±0.32, 0.84±0.16 and 0.80±0.17, respectively, for predicting lymph node positivity and 0.45±0.08, 0.79±0.06 and 0.63±0.05 for predicting distant metastases using a CNN in 264 subjects with non-small cell lung cancer (30).

In addition, AI has been used for disease classification, localization and volumetric assessment. Often, algorithm performance improves when more input data or data types are used. For example, Sibille et al. investigated a deep CNN to localize and classify [^{18}F]FDG uptake in lung cancer patients, based on whole-body PET/CT (31). In this study, the network structure (Fig. 2) combined convolutional and fully connected (dense) layers, and used a number of input modalities (PET, CT, maximum intensity projection (MIP), and atlas position), to produce two output decisions; node classification and localization. For the lung cancer patients, this approach gave 87% sensitivity and 99% specificity for classification, with localization accuracy of 97% (body part), 84% (organ/tissue), and 89% (subregion/ nodal station). Hyun et al. compared several algorithms such as random forests, neural networks and support vector machines, among others, to classify pathology in a sample of 396 subjects, 210 with adenocarcinoma and 186 with squamous cell carcinoma (32). Interestingly, the authors found that a comparatively simple logistic regression model outperformed all other classifiers with accuracy estimated at 77%.

Since certain features, such as heterogeneity, are associated with an increased risk of malignancy, work has also been done investigating the use of texture-based analysis to determine risk stratification. Sometimes, texture features are used to classify a lesion as benign or malignant. *Radiomics,* in combination with AI, tries to identify previously unknown imaging features based on review of mathematical patterns and pattern combinations. Further texture features that might not be easily quantifiable by the human eye can be extracted from images, quantified and then used to aid with disease characterization and classification. A study by Zhang et al. of 135 patients with PET/CT used radiomic features on CT and metabolic parameters on PET to classify benign from malignant lung lesions across a spectrum of pathology. The authors found an AUC of 0.887±0.046 with accuracy, sensitivity and specificity of 0.815±0.066, 0.814±0.058 and 0.816±0.079,

respectively (33). There is the suggestion that AI algorithms may reduce unnecessary follow-up (34-38). Regardless of AI algorithm used, however, it is important to remember that tissue sampling remains key for disease confirmation. Also, one of the challenges that remains is having access to sufficient data to capture the disease spectrum without overfitting for a specific cohort.

Understanding the genetic and pathobiological underpinnings of lung cancer contributes to precision medicine by influencing the decision to treat and the type of treatment to give (39,40). Ultimately large prospective studies are needed to confirm utility of AI in clinical practice in this arena. Although standardization efforts for feature extraction have been made (41), standardization in image acquisition, reconstruction, and segmentation, among other things, is also needed. We are in the early days of the application of AI to clinical practice and transparent reporting of the data used and algorithm design remains essential for the assessment of reproducibility and to provide fair comparisons (34, 42).

Current Clinical Value of PET and AI in Lung Cancer Treatment Strategy

PET is helpful to detect and characterize lung cancer, both at initial staging as well as for subsequent treatment strategy development. Metrics measured from PET images, such as baseline intensity and extent of radiopharmaceutical uptake as well as change in these metrics with therapy, can be used as *predictive biomarkers* of response to therapy as well as a *biomarkers of prognosis*. According to the Society for Nuclear Medicine and Molecular Imaging, [^{18}F]FDG-PET/CT is appropriate for: 1) restaging patients with lung cancer after treatment, 2) detection of recurrence, and 3) treatment response evaluation (43).

Utility of AI in conjunction with PET in lung cancer follow-up:

While preliminary investigations suggest AI may be a helpful tool in the lung cancer treatment algorithm, to date, the available data remains limited. In this section, we highlight a few studies to illustrate the spectrum of what is being studied.

Buizza et al. used image features on PET/CT scans acquired at baseline and after 3 weeks of chemoradiotherapy in conjunction with linear support vector machines in 30 patients with NSCLC to predict survival (44). Mattonen et al. also used image features on PET/CT scans in conjunction with a linear regression model to predict survival in patients with NSCLC (45). While different algorithms have been assayed with varying results, ultimately multi-variable multi-step models may give among the best results. For example, a paper by Baek et al. appeared promising.

In this paper, a sophisticated multi-step AI model (Fig. 3), referred to as a deep segmentation network, was trained to predict survival in patients with NSCLC (46). Using cross-validation experiments on a data set with 96 NSCLC cases, the AUC was 0.88 when predicting 2-year overall survival, representing an improvement over other techniques that produce AUC values ranging from 0.60 to 0.83 over the same data set. The AI model consisted of supervised U-nets, followed by unsupervised k-medoids clustering, and then supervised logistic regression. Contrary to the more conventional approach where a CNN would be directly trained with survival data, in this paper, the U-nets were trained for segmentation using physician-drawn regions of interest (ROIs), and separate networks for CT and PET data. Intermediate results from the U-nets, taken from the middle encoded (i.e., feature-space) layers, were used as input to the clustering algorithm. The authors showed that by training the U-nets in this manner, the intermediate features conveyed more structural information than the textural information which is more prevalent in a network trained directly with survival data. Results from the k-medoids algorithm were used to identify key features that were then fed into the supervised logistic regression algorithm, trained using survival data.

Tseng et al. used generative adversarial networks (GANs) as part of the treatment planning for NSCLC to automate radiation adaptation to good effect (Fig. 4) (47).

Conclusion

AI in conjunction with PET, though still in its infancy, has the potential to become an integral decision-making tool in the precision medicine algorithm of lung cancer patients. PET coupled with either CT or MRI provides anatmo-molecular insight during the course of lung cancer patient care. AI can use this the information derived from this imaging to assist with staging, treatment planning, and outcome prediction.

References

[1] American Cancer Society. Key Statistics for Lung Cancer. Updated December, 2020. Available: <http://www.cancer.org/cancer/lungcancer-non-smallcell/detailedguide/non-small-cell-lung-cancer-key-statistics>.

[2] Herbst RS, Morgensztern D, Boshoff C. The biology and management of non-small cell lung cancer. Nature. 2018; 553:446-454.

[3] Mena E, Yanamadala A, Cheng G, et al. The Current and Evolving Role of PET in Personalized Management of Lung Cancer. PET Clin. 2016; 11(3):243-59.

[4] Warburg O, Wind F, Negelein E. The Metabolism of Tumours in the Body. J Gen Physiol. 1927; 8(6):519–30.

[5] Warburg O. On Respiratory Impairment in Cancer Cells. Science. 1956; 124(3215):269–70.
[6] Kinoshita T, Fujii H, Hayashi Y, et al. Prognostic significance of hypoxic PET using (18)F-FAZA and (62)Cu-ATSM in non-small-cell lung cancer. Lung Cancer. 2016; 91:56-66.
[7] Giesel FL, Adeberg S, Syed M, et al. FAPI-74 PET/CT using either 18F-AIF or cold-kit 68Ga-labeling: biodistribution, radiation dosimetry and tumor delineation in lung cancer patients. J Nucl Med [Epub ahead of print].
[8] Gould MK, Tang T, Liu IL, et al. Recent Trends in the Identification of Incidental Pulmonary Nodules. Am J Respir Crit Care Med. 2015; 192(10):1208-14.
[9] MacMahon H, Naidich DP, Goo JM, et al. Guidelines for Management of Incidental Pulmonary Nodules Detected on CT Images: From the Fleischner Society 2017. Radiology. 2017; 284(1):228-243.
[10] Gould MK, Maclean CC, Kuschner WG, Rydzak CE, Owens DK. Accuracy of Positron Emission Tomography for Diagnosis of Pulmonary Nodules and Mass Lesions: a Meta-Analysis. JAMA. 2001; 287:914–24.
[11] Gambhir SS, Czernin J, Schwimmer J, Silverman DH, Coleman RE, Phelps ME. A Tabulated Summary of the FDG PET Literature. J Nucl Med. 2001; 42:1S–93S.
[12] Cronin P, Dwamena B, Kelly AM, Carlos RC. Solitary Pulmonary Nodules: Meta-Analytic Comparison of Cross-Sectional Imaging Modalities for Diagnosis of Malignancy. Radiology. 2008; 246:772–82.
[13] Garcia-Velloso MJ, Bastarrika G, de-Torres JP, et al. Assessment of Indeterminate Pulmonary Nodules Detected in Lung Cancer Screening: Diagnostic Accuracy of FDG PET/CT. Lung Cancer. 2016; 97:81-6.
[14] Fletcher JW, Djulbegovic B, Soares HP, et al. Recommendations on the Use of ^{18}F-FDG PET in Oncology. J Nucl Med. 2008; 49(3):480–508.
[15] Lardinois D, Weder W, Hany TF, et al. Staging of Non–Small-Cell Lung Cancer with Integrated Positron Emission Tomography and Computed Tomography. N Engl J Med. 2003; 348:2500–7.
[16] Gerbaudo VH, Julius B. Anatomo-Metabolic Characteristics of Atelectasis in F-18 FDG-PET/CT Imaging. Eur J Radiol. 2007; 64(3):401–5.
[17] Gould MK, Kuschner WG, Rydzak CE, et al. Test Performance of Positron Emission Tomography and Computed Tomography for Mediastinal Staging in Patients with Non-Small-Cell Lung Cancer: a Meta-Analysis. Ann Intern Med. 2003; 139:879–92.
[18] Fischer BM, Mortensen J, Hansen H, et al. Multimodality Approach to Mediastinal Staging in Non-Small Cell Lung Cancer. Faults and Benefits of PET-CT: A Randomised Trial. Thorax. 2011;

66(4):294–300.
[19] Hellwig D, Ukena D, Paulsen F, Bamberg M, Kirsch CM, Onko-PET der Deutschen Gesellschaft fur Nuklearmedizin. Meta-Analysis of the Efficacy of Positron Emission Tomography with F-18-Fluorodeoxyglucose in Lung Tumors. Basis for Discussion of the German Consensus Conference on PET in Oncology 2000. Pneumologie. 2001; 55(8):367–77.
[20] MacManus MP, Hicks RJ, Matthews JP, et al. High Rate of Detection of Unsuspected Distant Metastases by PET in Apparent Stage III Non-Small-Cell Lung Cancer: Implications for Radical Radiation Therapy. Int J Radiat Oncol Biol Phys. 2001; 50(2):287–93.
[21] Uribe CF, Mathotaarachchi S, Gaudet V, et al. Machine Learning in Nuclear Medicine: Part 1-Introduction. J Nucl Med. 2019; 60(4):451-458.
[22] Armato SG 3rd, McLennan G, Bidaut L, et al. The Lung Image Database Consorium (LIDC) and Image Database Resource Initiative (IDRI): a completed reference database of lung nodules on CT scans. Med Phys. 2011; 38(2):915-931.
[23] Aberle DR, Adams AM, et al. Reduced lung-cancer mortality with low-dose computed tomographic screening. N Engl J Med. 2011; 365(5):395-409.
[24] Zhao YR, Xie X, de Koning HJ, et al. NELSON lung cancer screening study. Cancer Imaging. 2011; 11 Spec No AS75-84.
[25] Yang Y, Feng X, Chi W, et al. Deep learning aided decision support for pulmonary nodules diagnosing: a review. J Thorac Dis. 2018; 10 (Suppl. 7):S867-S875.
[26] Schwyzer M, Martini K, Benz DC, et al. Artificial intelligence for detecting small FDG-positive lung nodules in digital PET/CT: impact of image reconstructions on diagnostic performance. Eur Radiol. 2020; 30(4):2031-2040.
[27] Schwyzer M, Ferraro DA, Muehlematter UJ, et al. Automated detection of lung cancer at ultralow dose PET/CT by deep neural networks – Initial results. Lung Cancer. 2018; 126:170-173.
[28] Zhao X, Li L, Lu W, Tan S. Tumor Co-Segmentation in PET/CT using Multi-Modality Fully Convolutional Neural Network. Phys Med Biol. 2020; 64(1):015011.
[29] Kirienko M, Sollini M, Silvestri G, et al. Convolutional neural networks promising in lung cancer T-parameter assessment on baseline FDG-PET/CT. Contrast Media Mol Imaging. 2018; 1382309.
[30] Tau N, Stundzia A, Yasufuku K, et al. Convolutional neural networks in predicting nodal and distant metastatic potential of newly diagnosed non-small cell lung cancer on FDG PET images. AJR Am J Roentgenol. 2020; 1-6.
[31] Sibille L, Seifert R, Avramovic N, et al. 18F-FDG PET/CT Uptake Classification in Lymphoma and Lung Cancer by Using Deep Convolutional Neural Networks. Radiology. 2020;

294:445-452.
[32] Hyun SH, Ahn MS, Koh YW, et al. A machine-learning approach using PET-based radiomics to predict the histologic subtypes of lung cancer. Clin Nucl Med. 2019; 44(12):956-960.
[33] Zhang R, Zhu L, Cai Z, et al. Potential feature exploration and model development based on 18F-FDG PET/CT images for differentiating benign and malignant lung lesions. Eur Radiol. 2019; 121:108735
[34] Zukotynski K, Gaudet V, Uribe CF, et al. Machine Learning in Nuclear Medicine: Part 2-Neural Networks and Clinical Aspects. J Nucl Med. 2021; 62(1):22-29.
[35] Kang G, Liu K, Hou B, et al. 3D multi-view convolutional neural networks for lung nodule classification. PLoS One. 2017; 12(11):e0188290
[36] Xie Y, Xia Y, Zhang J, et al. Knowledge-based collaborative Deep learning for benign-malignant lung nodule classification on chest CT. IEEE Trans Med Imaging. 2019; 38(4):991-1004.
[37] Nibali A, He Z, Wollersheim D. Pulmonary nodule classification with deep residual networks. Int J Comput Assis Radiol Surg. 2017; 12(10):1799-808.
[38] da Silva GLF, Valente TLA, Silva AC, et al. Convolutional neural network-based PSO for lung nodule false positive reduction on CT images. Comput Methods Programs Biomed. 2018; 162109-18.
[39] Manafi-Farid R, Karamzade-Ziarati N, Vali R, et al. 2-[18F]FDG PET/CT radiomics in lung cancer: An overview of the technical aspect and its emerging role in management of the disease. Methods. 2020; S1046-2023(19)30325-1.
[40] Yang SR, Schultheis AM, Yu H, et al. Precision medicine in non-small cell lung cancer: Current applications and future directions. Semin Cancer Biol. 2020;S1044-579X(20)30164-4.
[41] Zwanenburg A, Vallières M, Abdalah MA, et al. The Image Biomarker Standardization Initiative: Standardized Quantitative Radiomics for High-Throughput Image-based Phenotyping. Radiology. 2020; 295(2):328-338.
[42] Park H, Sholl LM, Hatabu H, et al. Imaging of Precision Therapy for Lung Cancer: Current State of the Art. Radiology 2019; 293:15-29.
[43] Jadvar H, Colletti PM, Delgado-Bolton R, et al. Appropriate use criteria for 18F-FDG PET/CT in restaging and treatment response assessment of malignant disease. J Nucl Med. 2017; 58(12): 2026-2037.
[44] Buizza G, Toma-Dasu I, Lazzeroni M, et al. Early tumor response prediction for lung cancer patients using novel longitudinal pattern features from sequential PET/CT image scans. Phys Med. 2018;54:21-29.

[45] Mattonen SA, Davidzon GA, Benson J, et al. Bone marrow and tumor radiomics at 18F-FDG PET/CT: impact on outcome prediction in non-small cell lung cancer. Radiology. 2019;293(2): 451-459.
[46] Baek S, He Y, Allen BG, et al. Deep segmentation networks predict survival of non-small cell lung cancer. Sci Rep. 2019; 9:17286.
[47] Tseng HH, Luo Y, Cui S, Chien JT, Ten Haken RK, El Naqa I. Deep Reinforcement Learning for Automated Radiation Adaptation in Lung Cancer. Med Phys. 2017; 44(12):6690-6705.

Figure Legends:

Figure 1. Illustration of the network used by Zhao et al. to segment lung cancer based on PET/CT with V-net style 3D fully convolutional neural network (FCN) and feature fusion (28). The CNNs create feature maps for each input (PET/CT). These feature maps are concatenated and undergo feature re-extraction to produce a fused feature map.

Figure 2. Illustration of the network used by Sibille et al. for the purpose of localization and classification in patients with lung cancer or lymphoma (31). Note that the model uses a combination of inputs (PET, CT, position of cropped region, maximum intensity projection (MIP)), and types of layers (convolutional, fully connected).

Figure 3. Illustration of the network used by Baek et al. for the purpose of predicting survival in patients with non-small cell lung cancer (46). A) Simplified structure of a deep segmentation network to predict the likelihood of survival from NSCLC. The structure used for training included a U-Net (simplified here to 5 layers), k-medoids clustering, LASSO feature selection, and logistic regression. B) The structure used for online operation, which includes the U-Net encoder, selection of p relevant features, and logistic regression.

Figure 4. Illustration of the network used by Tseng et al. for the purpose of radiation therapy planning in patients with non-small cell lung cancer (47). The framework used consisted of 3 parts: a Generative Adversarial Network (GAN), a Radiotherapy Artificial Environment (RAE) and a Deep Q-Network (DQN). A) A total of 297 variables were collected using the PET/CT, clinical factors, etc., with 9 variables selected using Markov Blankets and Bayesian statistics. The GAN was used to generate synthetic patient data. B) Real and synthesized patient data were used to estimate transition probabilities regarding radiation response such as pneumonitis and local control prediction factors. The transition probabilities make up the RAE, which produces a reward in response to the action taken by the optimal policy learned from the DQN.

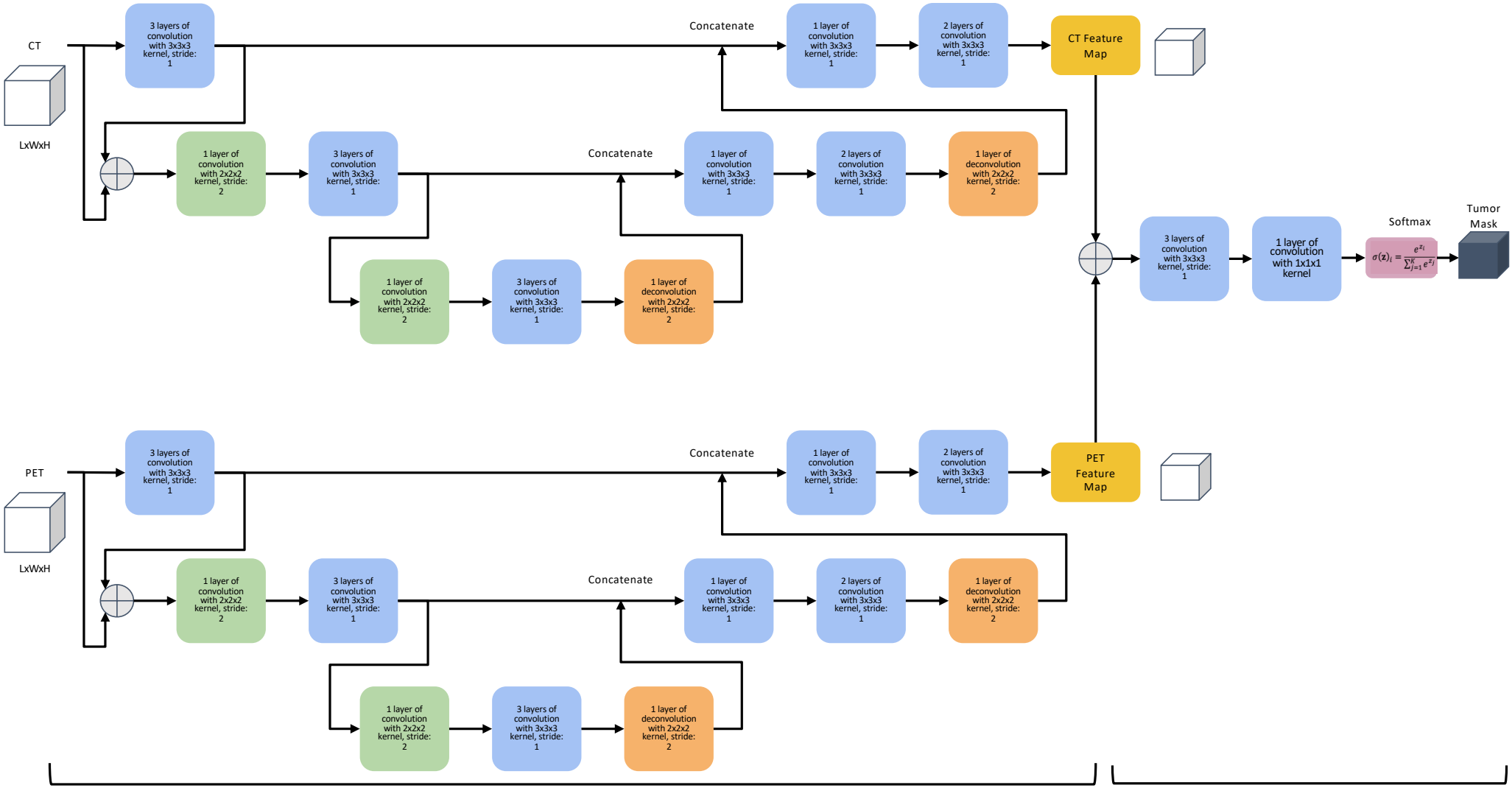
CT
LxWxH
3 layers of convolution with 3x3x3 kernel, stride: 1
Concatenate
1 layer of convolution with 3x3x3 kernel, stride: 1
2 layers of convolution with 3x3x3 kernel, stride: 1
CT Feature Map
1 layer of convolution with 2x2x2 kernel, stride: 2
3 layers of convolution with 3x3x3 kernel, stride: 1
Concatenate
1 layer of convolution with 3x3x3 kernel, stride: 1
2 layers of convolution with 3x3x3 kernel, stride: 1
1 layer of deconvolution with 2x2x2 kernel, stride: 2
1 layer of convolution with 2x2x2 kernel, stride: 2
3 layers of convolution with 3x3x3 kernel, stride: 1
1 layer of deconvolution with 2x2x2 kernel, stride: 2
3 layers of convolution with 3x3x3 kernel, stride: 1
1 layer of convolution with 1x1x1 kernel
Softmax
$\sigma(\mathbf{z})_i = \frac{e^{z_i}}{\sum_{j=1}^{K} e^{z_j}}$
Tumor Mask
PET
LxWxH
3 layers of convolution with 3x3x3 kernel, stride: 1
Concatenate
1 layer of convolution with 3x3x3 kernel, stride: 1
2 layers of convolution with 3x3x3 kernel, stride: 1
PET Feature Map
1 layer of convolution with 2x2x2 kernel, stride: 2
3 layers of convolution with 3x3x3 kernel, stride: 1
Concatenate
1 layer of convolution with 3x3x3 kernel, stride: 1
2 layers of convolution with 3x3x3 kernel, stride: 1
1 layer of deconvolution with 2x2x2 kernel, stride: 2
1 layer of convolution with 2x2x2 kernel, stride: 2
3 layers of convolution with 3x3x3 kernel, stride: 1
1 layer of deconvolution with 2x2x2 kernel, stride: 2
V-Net style Architecture
Feature Fusion Network

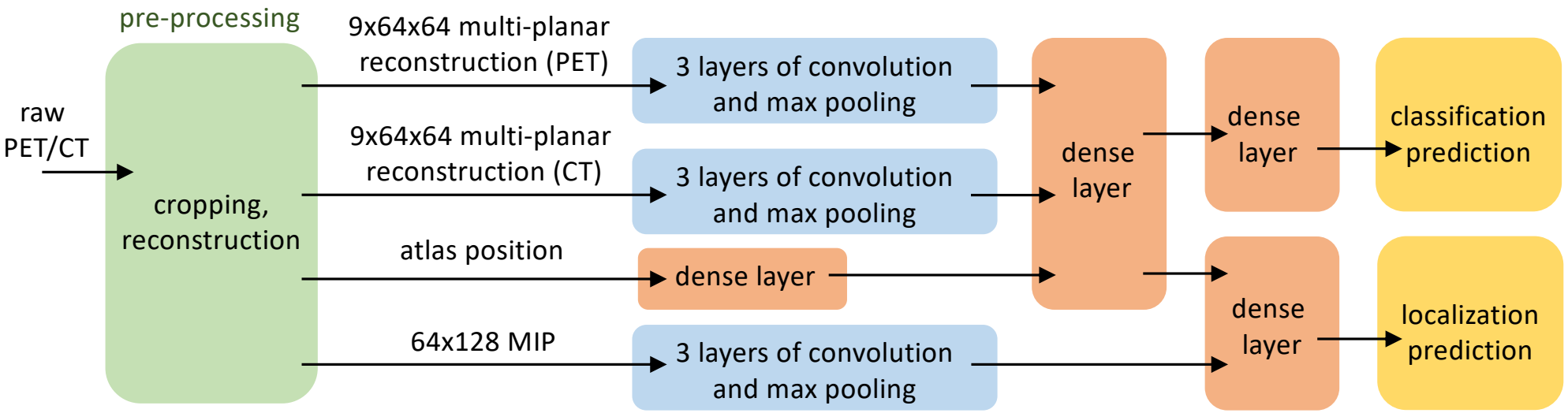
pre-processing
raw
PET/CT
cropping,
reconstruction
9x64x64 multi-planar
reconstruction (PET)
9x64x64 multi-planar
reconstruction (CT)
atlas position
64x128 MIP
3 layers of convolution
and max pooling
3 layers of convolution
and max pooling
dense layer
3 layers of convolution
and max pooling
dense
layer
dense
layer
classification
prediction
dense
layer
localization
prediction

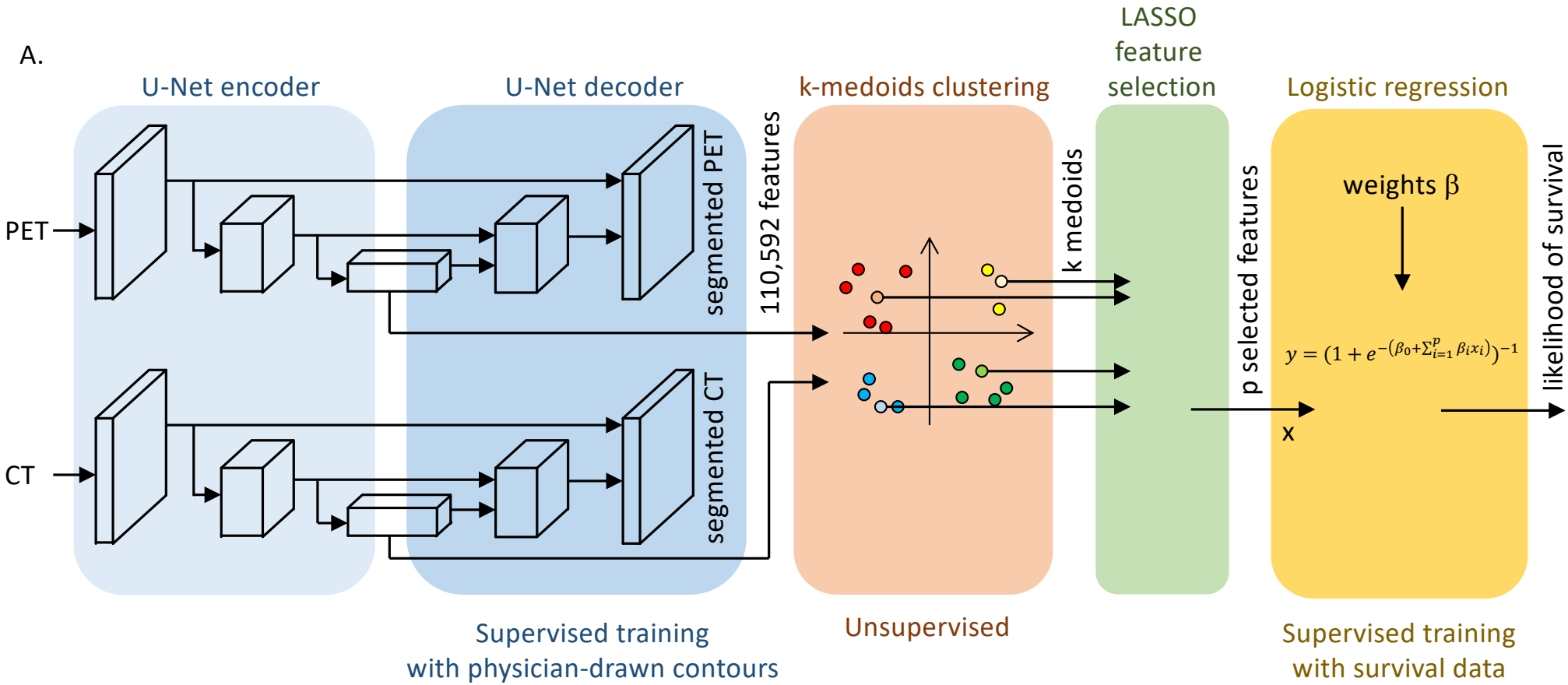
A.
U-Net encoder
U-Net decoder
k-medoids clustering
LASSO feature selection
Logistic regression
PET
CT
segmented PET
segmented CT
110,592 features
k medoids
p selected features
x
weights β
$y = (1 + e^{-(\beta_0 + \sum_{i=1}^{p} \beta_i x_i)})^{-1}$
likelihood of survival
Supervised training with physician-drawn contours
Unsupervised
Supervised training with survival data

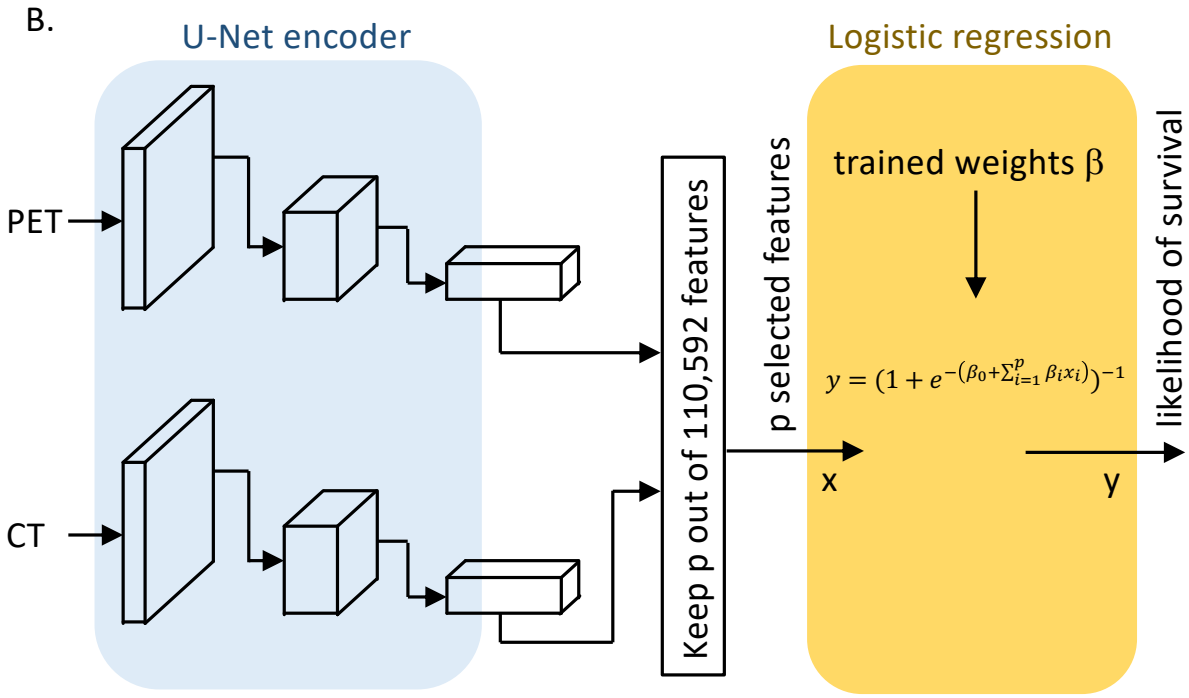
B.
U-Net encoder
Logistic regression
PET
CT
Keep p out of 110,592 features
p selected features
trained weights β
$y = (1 + e^{-(\beta_0 + \sum_{i=1}^{p} \beta_i x_i)})^{-1}$
x
y
likelihood of survival

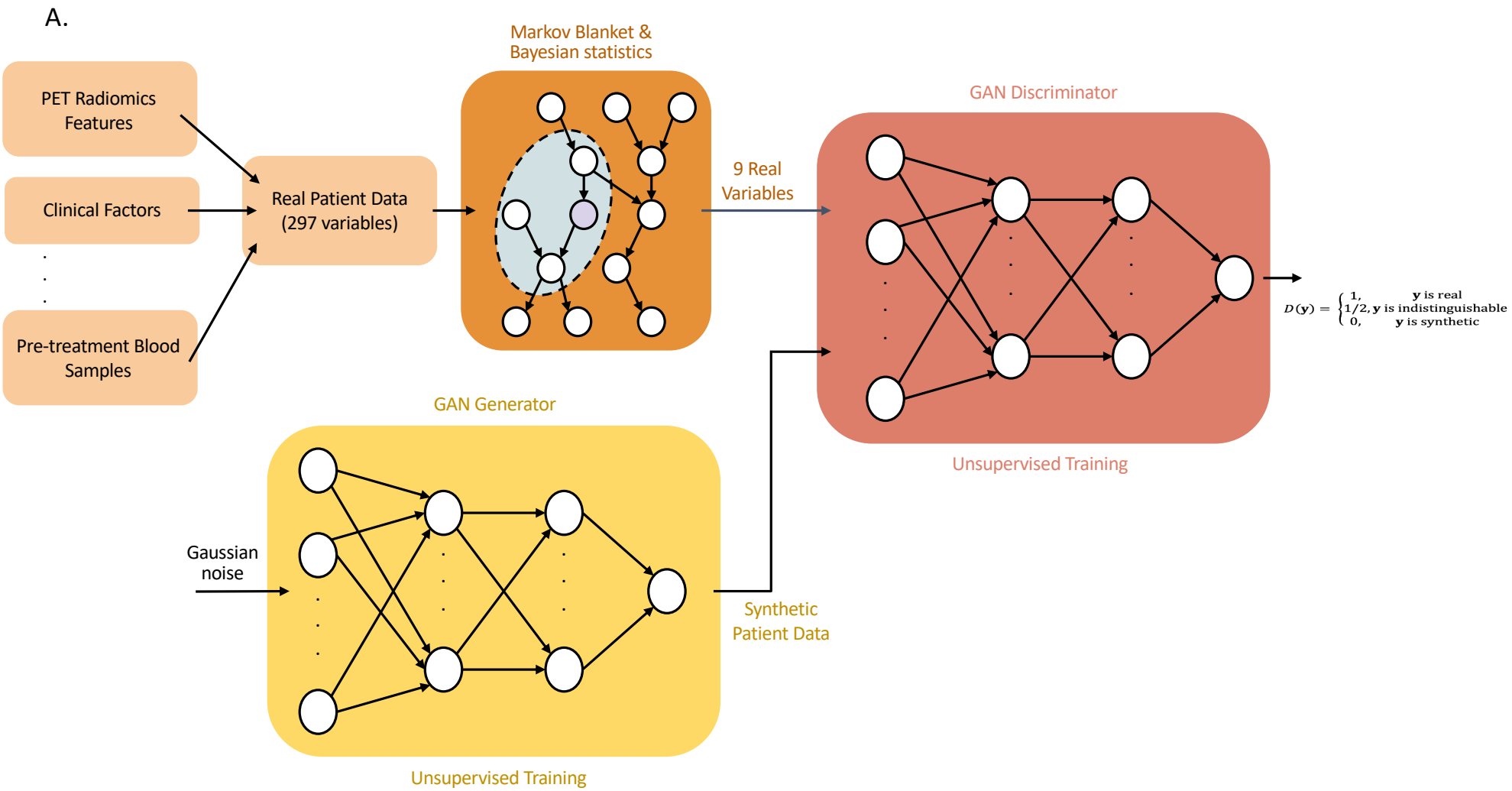
A.
PET Radiomics Features
Clinical Factors
Pre-treatment Blood Samples
Real Patient Data (297 variables)
Markov Blanket & Bayesian statistics
9 Real Variables
GAN Discriminator
$D(\mathbf{y}) = \begin{cases} 1, & \mathbf{y} \text{ is real} \\ 1/2, & \mathbf{y} \text{ is indistinguishable} \\ 0, & \mathbf{y} \text{ is synthetic} \end{cases}$
Unsupervised Training
GAN Generator
Gaussian noise
Synthetic Patient Data
Unsupervised Training

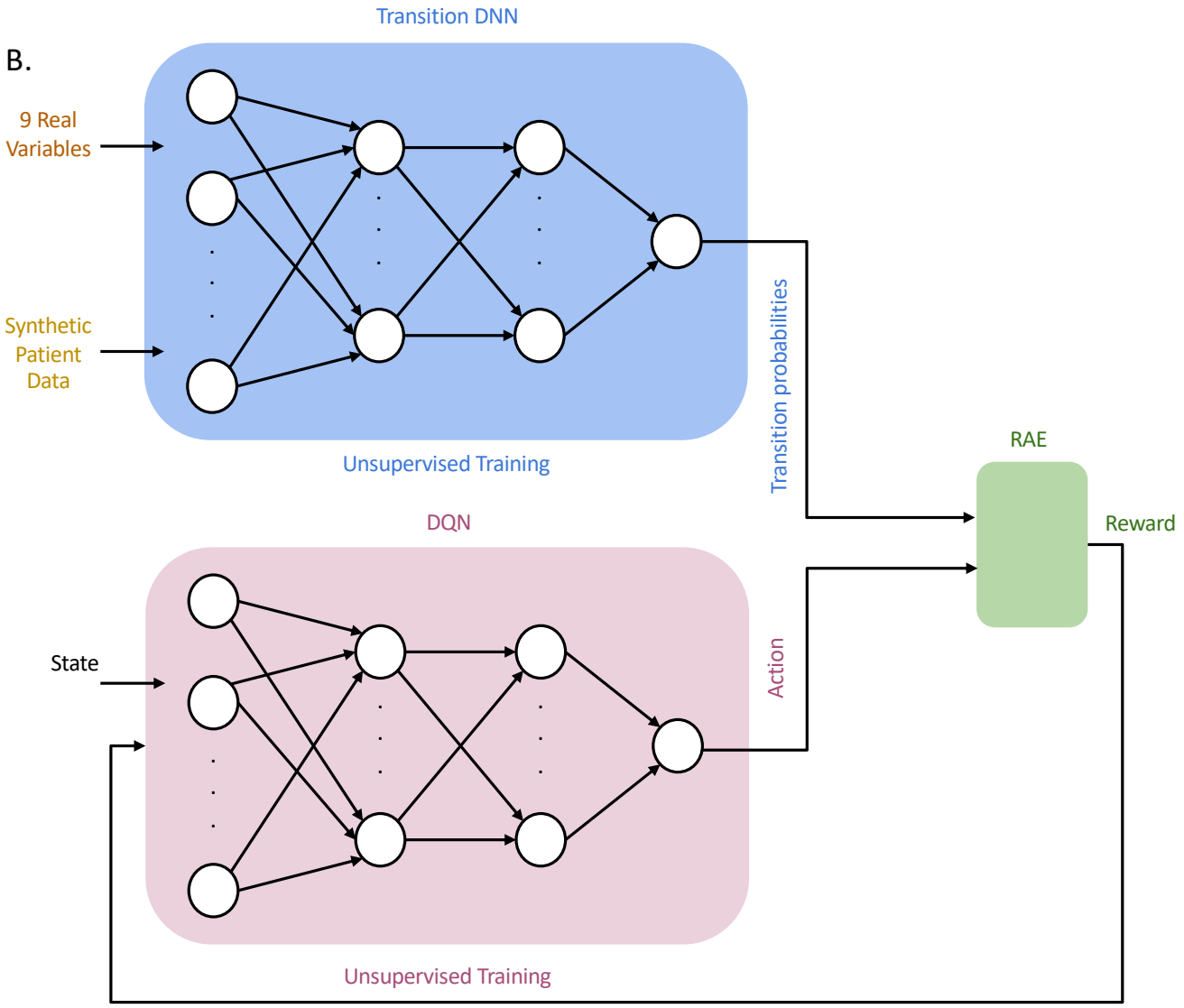
B.
Transition DNN
9 Real Variables
Synthetic Patient Data
Unsupervised Training
Transition probabilities
RAE
Reward
DQN
State
Action
Unsupervised Training